Supplementary Figure 1. *Jussila et al.*

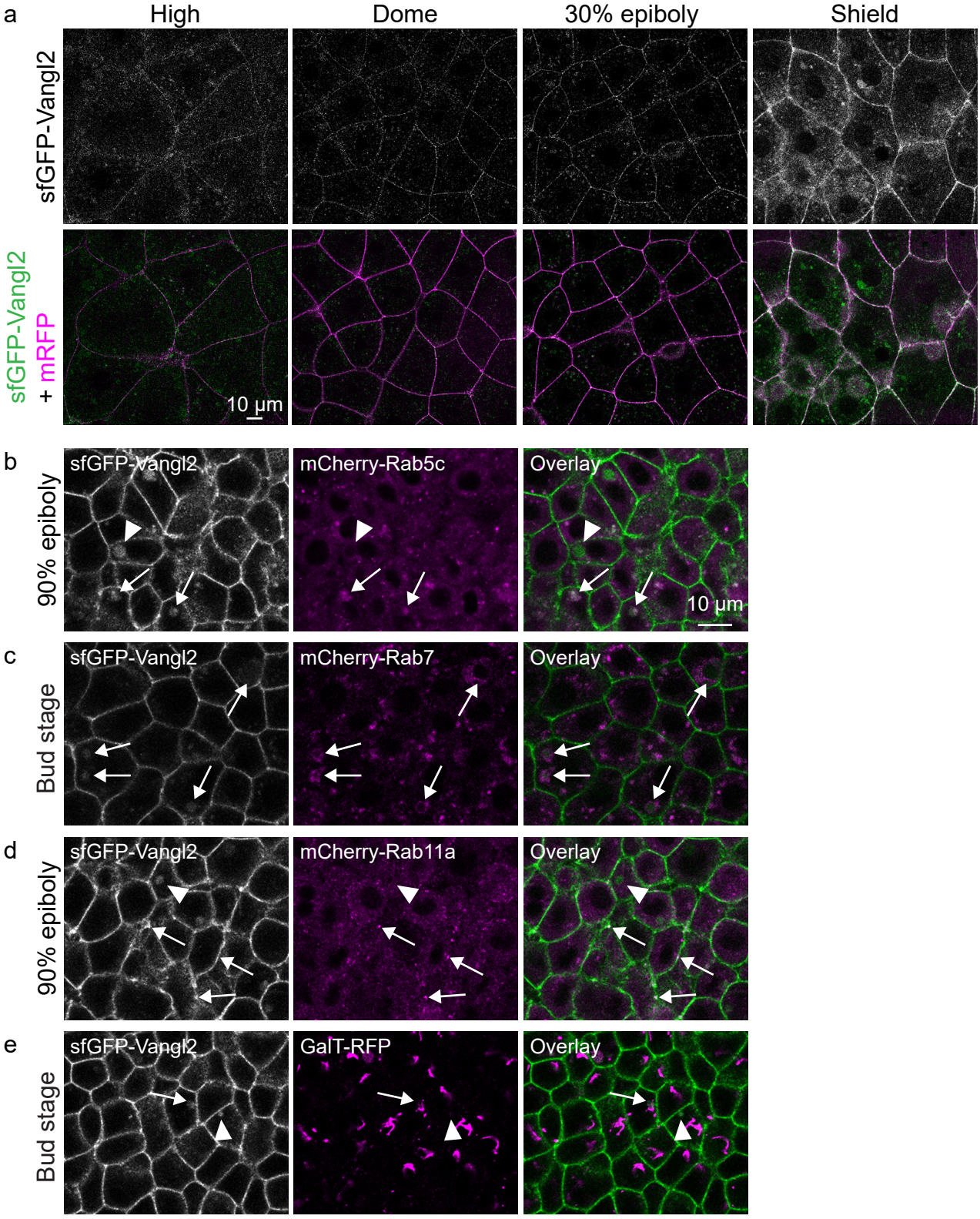

Supplementary Figure 1. Vangl2 shows membrane-localization during early zebrafish development with cytoplasmic Vangl2 colocalizing with Rab7

(a) Live confocal images of EVL cells of *vangl2*^{sfGFP} embryos at blastula and early gastrula stages. Embryos were injected with mRNA coding for a membrane-localized monomeric RFP (mRFP) reporter. All sfGFP images were acquired using identical settings.

(b-e) Live confocal images of ectodermal cells between dorsal and lateral domains in 90% epiboly or bud staged *vangl2*^{sfGFP} embryos at injected with mRNA coding for mCherry-Rab5c (b), mCherry-Rab7 (c), mCherry-Rab11a (d) or GalT-RFP (e) reporters. Arrows point at cytoplasmicVangl2 puncta in close proximity to respective reporters, and arrowheads point at isolated Vangl2 puncta.

Supplementary Figure 2. *Jussila et al.*

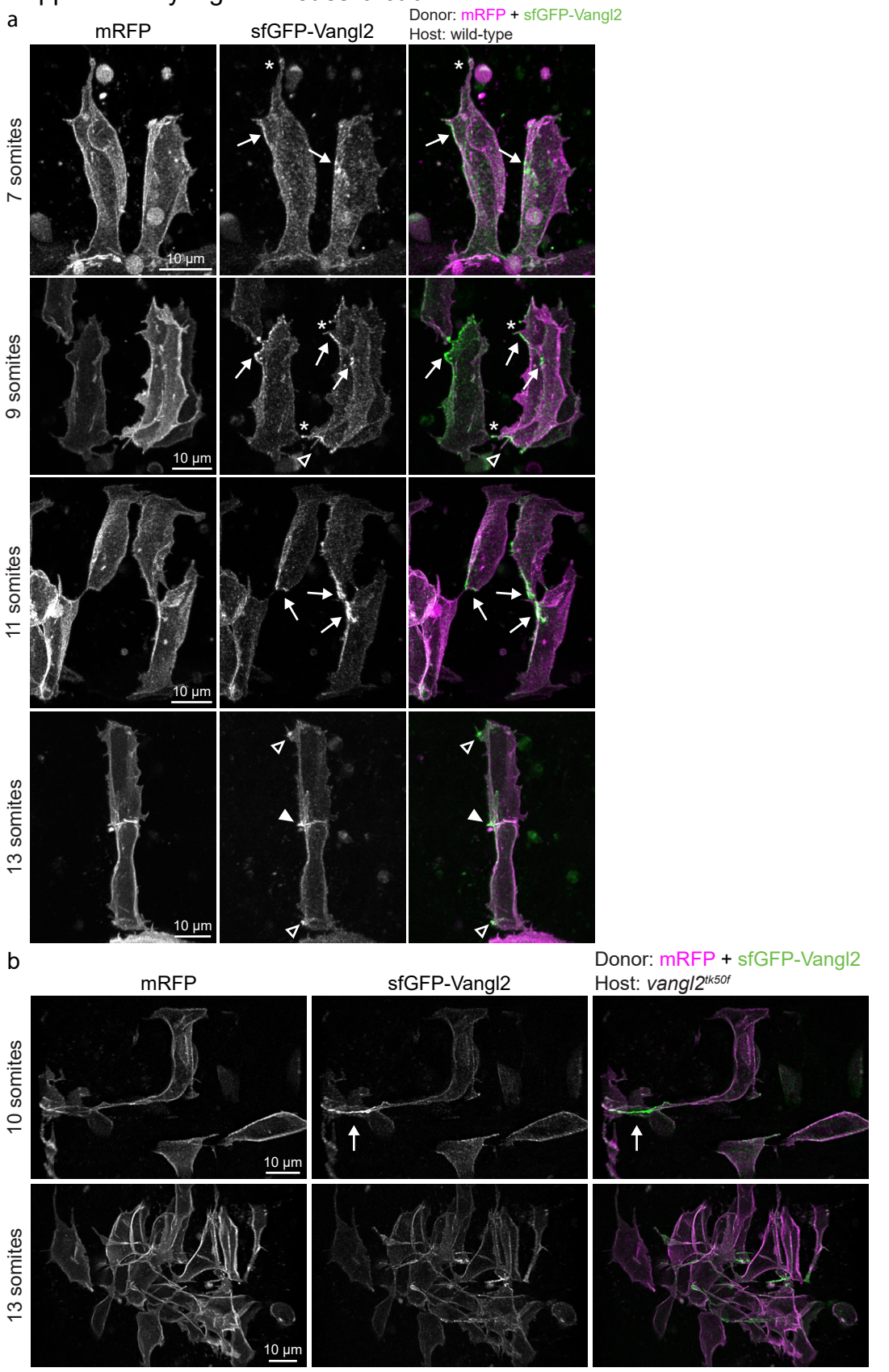

Supplementary Figure 2. Vangl2 is enriched on anterior membranes of neuroepithelial cells and is membrane-localized but not polarized in a PCP deficient environment

(a) Confocal images of mRFP and sfGFP-Vangl2 localization in the developing spinal cord of chimeric embryos (*mRFP* mRNA-injected *vangl2*^{sfGFP} cells transplanted into wild-type hosts) at progressive stages of neural tube morphogenesis. Maximum intensity projections are shown, anterior is to the left. Arrows point at Vangl2 enrichment on cell membranes, arrowheads at apical membranes at the neural midline, open arrowheads at Vangl2 enrichment on basal membranes, and asterisks at Vangl2-positive cell protrusions.

(b) Confocal images of mRFP and sfGFP-Vangl2 localization in transplanted *vangl2*^{sfGFP} neuroepithelial cells within *vangl2*^{tk50f} mutant hosts, at 10-somite and 13-somite stages of development. Maximum intensity projections are shown, anterior is to the left. Arrow points at Vangl2 enrichment to a membrane protrusion.

Supplementary Figure 3. *Jussila et al.*

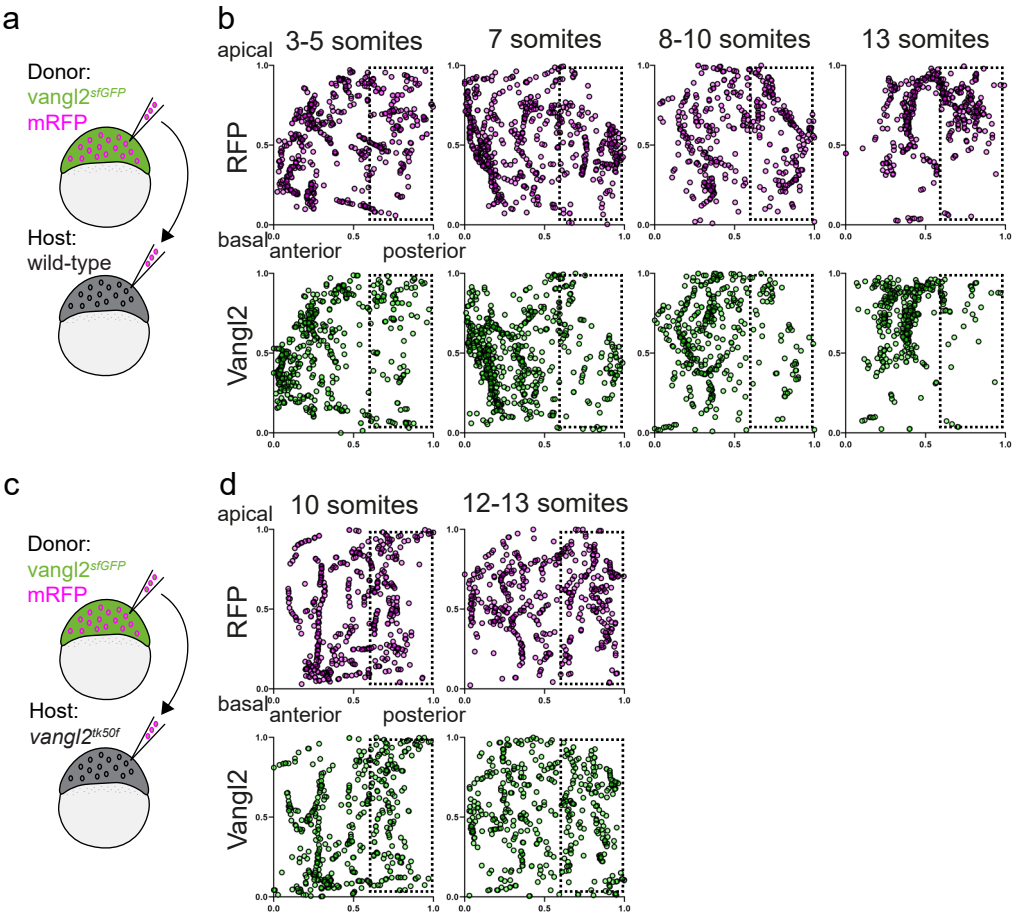

Supplementary Figure 3. Quantification of Vangl2 localization shows that it is anteriorly enriched and requires functional PCP for its polarization.

(a) A schematic illustrating cell transplantation from a membrane-RFP labelled *vangl2*^{sfGFP} donor embryo into a wild-type host embryo at sphere stage.

(b) Scatter plots showing the distribution of the brightest sfGFP-Vangl2 and membrane-RFP spots along anterior-posterior (X) and apical-basal (Y) axes of *vangl2*^{sfGFP} neuroepithelial cells, quantified at four consecutive stages of neural tube morphogenesis. Data from multiple transplanted *vangl2*^{sfGFP} cells was pooled (3-5 somites, n = 7; 7 somites, n = 7; 8-10 somites, n = 6; 13 somites, n = 5) and axial lengths normalized to 1. Details of the quantification can be found in the Methods section.

(c) A schematic illustrating cell transplantation from a membrane-RFP labelled *vangl2*^{sfGFP} donor embryo into a *vangl2*^{tk50f} host embryo at sphere stage.

(d) Scatter plots showing the distribution of the brightest Vangl2 and membrane-RFP spots along anterior-posterior (X) and apical-basal (Y) axes of *vangl2*^{sfGFP} neuroepithelial cells in a *vangl2*^{tk50f} mutant host, quantified at two consecutive stages of neural tube morphogenesis. Data from multiple transplanted *vangl2*^{sfGFP} cells was pooled (10 somites, n = 7; 12-13 somites, n = 9).

Supplementary Figure 4. *Jussila et al.*

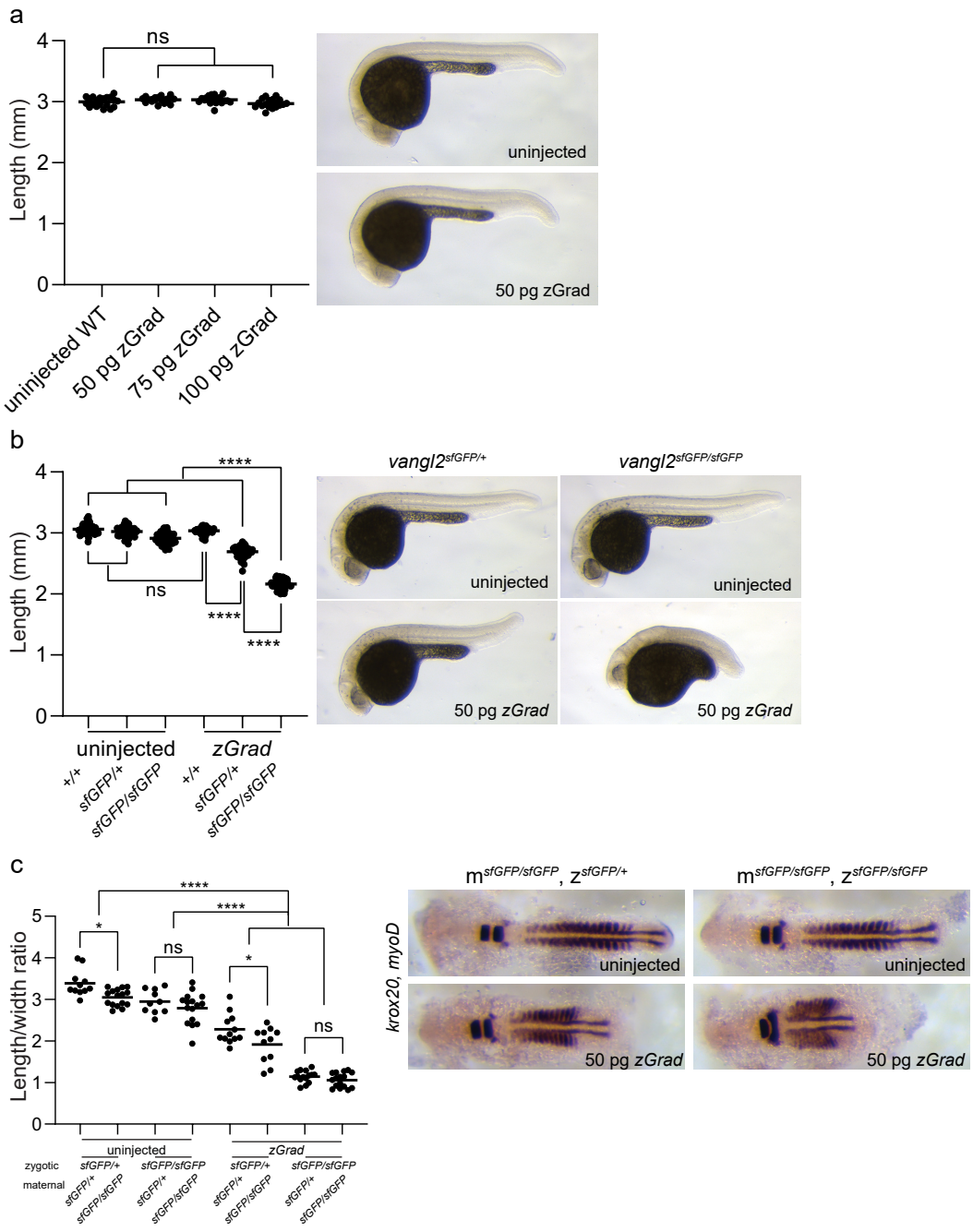

Supplementary Figure 4. Optimizing zGrad GFP-nanobody protein degradation methodologies to disrupt sfGFP-Vangl2 function

(a) Quantification of 24 hpf embryo lengths following *zGrad* mRNA injection into wild-type embryos. Data shows one of two performed experiments. Statistical analysis was performed using one-way ANOVA with Tukey's multiple comparisons test. N=20 for each condition. Representative uninjected control embryos and 50 pg *zGrad* mRNA-injected embryos are shown in a lateral view.

(b) Quantification of 24 hpf embryo lengths following 50pg *zGrad* mRNA injection into embryos obtained from a *vangl2*$^{sfGFP/+}$ incross, genotypes are as indicated. Data is pooled together from two experiments. Statistical analysis was performed using one-way ANOVA with Tukey's multiple comparisons test (****P<0.0001). Control wild-type n=60, *vangl2*$^{sfGFP/+}$ n=60, *vangl2*$^{sfGFP/sfGFP}$ n=56, zGrad-injected wild-type n=43, *vangl2*$^{sfGFP/+}$ n=60, *vangl2*$^{sfGFP/sfGFP}$ n=48. Representative uninjected and 50 pg *zGrad* mRNA injected *vangl2*$^{sfGFP/+}$ and *vangl2*$^{sfGFP/sfGFP}$ embryos are shown in a lateral view.

(c) Quantification of length/width ratio of *zGrad* mRNA-injected and uninjected control embryos at 15 somite stages. Embryos obtained from crosses between *vangl2*$^{sfGFP/+}$ and *vangl2*$^{sfGFP/sfGFP}$ parents; maternal and zygotic *vangl2*^{sGFP} genotypes are as indicated. Statistical analysis was performed using two-way ANOVA with Tukey's multiple comparisons test (*P≤0.005, ****P<0.0001). Control n from left to right: n=11, n=16, n=10, n=16. zGrad n from left to right: n=12, n=11, n=15, n=16. Representative uninjected and 50 pg *zGrad* mRNA injected *vangl2*$^{sfGFP/+}$ and *vangl2*$^{sfGFP/sfGFP}$ embryos from *vangl2*$^{sfGFP/sfGFP}$ mothers are shown in a dorsal view. *krox20* and *myoD* expression were used to define hindbrain and somitic mesoderm boundaries, respectively, as detected by whole-mount RNA *in situ* hybridization.